Stimulating healthy tissue regeneration by targeting the 5-HT B receptor in chronic liver disease.

Mohammad R. Ebrahimkhani, Fiona Oakley, Lindsay B. Murphy, Jelena Mann, Anna Moles, Maria J. Perugorria, Elizabeth Ellis, Anne F. Lakey, Alastair D. Burt, Angela Douglass, et al.

Stimulating healthy tissue regeneration by targeting the 5-HT_{2B} receptor in chronic liver disease.

Mohammad R Ebrahimkhani[2,4], Fiona Oakley[1,4], Lindsay B Murphy[1], Jelena Mann[1], Anna Moles[1], Maria J Perugorria[1], Elizabeth Ellis[1], Anne F Lakey[1], Alastair Burt[1], Angela Douglass[1], Matthew C Wright[1], Steven A White[1], Fabrice Jaffré[3], Luc Maroteaux[3], and Derek A Mann[1].

[1] *Fibrosis Laboratory, Liver Group, Institute of Cellular Medicine, Newcastle University, Newcastle upon Tyne, NE24HH UK*.

[2] *MIT center for Environmental Health Sciences, Department of Biological engineering, Department of Biology, Massachusetts Institute of Technology (MIT), Cambridge, MA, USA*

[3]*INSERM UMR-S 839, F75005, Paris, France; Université Pierre et Marie Curie, F75005, Paris; Institut du Fer à Moulin, F75005, Paris.*

[4]*These two authors made an equal contribution to the work.*

Correspondence: E-mail: derek.mann@ncl.ac.uk.

Phone: +44 191 2223851

Fax: +44 191 2225455

Running title: 5-HT_{2B}R regulates hepatocyte proliferation and liver fibrosis.

INTRODUCTORY PARAGRAPH

Tissue homeostasis requires an effective, limited wound-healing response. In chronic disease, failure to regenerate parenchymal tissue leads to replacement of lost cellular mass with fibrotic matrix. The mechanisms that dictate the balance between cell regeneration and fibrogenesis are poorly understood. Here, we report in the liver that fibrogenic hepatic stellate cells (HSC) are negative regulators of hepatocyte regeneration. This function requires stimulation of 5-HT_{2B} receptors on HSC by serotonin, which activates expression of TGFβ1 (a powerful suppressor of hepatocyte proliferation) via ERK/JunD signalling. Selective antagonism of 5-HT_{2B} enhanced hepatocyte growth in models of acute and chronic liver injury, similar effects were observed in mice lacking 5-HT_{2B} or JunD and when HSC were selectively depleted. Antagonism of 5-HT_{2B} attenuated fibrogenesis and improved liver function in disease models in which fibrosis was pre-established and progressive. Pharmacological targeting of 5-HT_{2B} is safe in humans and may be therapeutic in chronic liver disease.

Diminished hepatocyte regeneration is a feature of liver disease and is associated with fibrogenesis leading to development of cirrhosis and cancer[1-3]. Regulation of hepatocyte proliferation is complex involving cross-talk between resident non-parenchymal cells and parenchymal cells, and recruited haematopoietic cells[4]. Due to this complexity, there is an incomplete understanding of how hepatocyte proliferation is regulated. As an example, the contribution of the hepatic stellate cell (HSC) is yet to be established[5]. In the diseased liver, HSC trans-differentiate into "activated" myofibroblasts that drive fibrogenesis by promoting net deposition of extracellular matrix[1,5]. HSC also secrete numerous soluble factors that may influence hepatocyte proliferation including hepatocyte growth factor (HGF), transforming growth factor β1 (TGFβ1) and interleukin-6 (IL-6)[1,5]. Previous studies suggested stimulatory functions for HSC in hepatocyte regeneration, however no conclusive *in vivo* evidence has been provided to date[6,7]. Since activated HSC are continually generated in diseased liver it is relevant to determine their influence on tissue regeneration.

Results

Hepatic stellate cells suppress liver regeneration.

Bile duct obstruction occurs in a variety of clinical settings and can cause cholestatic injury including hepatocyte death and fibrosis[8]. Bile duct ligation (BDL) is an established model of extrahepatic cholestasis in rodents[9]. We determined effects of depletion of HSC on hepatocyte proliferation in mice with ongoing progressive BDL-induced injury. This was achieved by targeted depletion of HSC in mice with pre-established BDL-induced disease. Selective *in vivo* depletion of activated αSMA+ HSC (fig 1a), was achieved by administration of the single chain antibody (scAb) C1-3 conjugated to gliotoxin which is a potent pro-apoptotic fungal metabolite[10,11,12]. It is important to note that the antigen specifically recognised by C1-3 is synaptophysin which is expressed on αSMA+ myofibroblasts derived from transdifferentiation of hepatic stellate cells but

is not detected on any other cellular source of αSMA+ cell in diseased rodent liver[13]. PCNA staining of liver sections revealed treatment with C1-3-gliotoxin stimulates hepatocyte proliferation (fig 1c). A control scAb-conjugate (CSBD9-gliotoxin) had no influence on hepatocyte proliferation and staining for F4/80 and CK19 confirmed no influence of C1-3-gliotoxin on numbers of Kupffer cells or cholangiocytes (fig 1b and supplementary fig 1). HSC depletion was not associated with changes in expression of the hedgehog target gene Gli2 ruling out activation of the hedgehog pathway as the mechanism by which apoptotic depletion of HSC stimulates hepatocyte growth (supplementary fig 1)[14].

5-HT_{2B} signalling dampens hepatocyte proliferation.

Platelet-derived serotonin (5-HT) regulates liver regeneration via the 5-HT_2 subclass (5-HT_{2A}, 5-HT_{2B} and 5-HT_{2C}) of serotonin receptors [15]. However, recently 5-HT has been shown to be produced by cholangiocytes and to limit biliary cell proliferation in an autocrine fashion[16], suggesting that 5-HT may exert different actions on a variety of liver cell types. We recently identified functional 5-HT_{2B} receptors on activated HSC in diseased liver[17]. SB204741 is a highly specific antagonist of 5-HT_{2B}, with negligible specificity for 5-HT_{2A} or 5-HT_{2C}[18]. Administration of SB204741 stimulated hepatocyte proliferation in progressive BDL-induced liver injury and acute carbon tetrachloride (CCl_4) induced liver damage (fig 1d,e). We observed no effect of SB204741 on expression of the hepatomitogen HGF (supplementary fig 2a), cholangiocyte proliferation and hedgehog signalling (supplementary fig 2b), and the selective 5-$HT_{2A/C}$ antagonist ketanserin was without effect on hepatocyte proliferation[19]. To confirm a repressive influence of 5-HT_{2B} signalling we compared hepatocyte proliferation in 5-HT_{2B} knockout and wild type mouse liver following partial hepatectomy. Uninjured 5-HT_{2B} knockout mice show no structural or biochemical evidence of liver defects (supplementary fig 3). Hepatocyte proliferation, measured by three independent protocols, was elevated in 5-HT_{2B} deficient mice at 36 and 72hrs

post-partial hepatectomy (figs 2a-c). IL-6 and TNFα are primers of hepatocyte regeneration expressed transiently within hours following surgery[4,20]; both were modestly increased in 5-HT_{2B} knockouts at 4hrs (fig 2d and e). TGFβ1 is induced in the termination phase of regeneration and functions as a repressor of hepatocyte proliferation[4,20]. TGFβ1 was induced at 36 hrs and remained elevated at 72 hrs post-surgery in wild type livers. However, TGFβ1 was not induced in 5-HT_{2B} knockout livers, instead if anything, expression was diminished at these time points compared with sham injured animals (fig 2f). To corroborate these data, we repeated partial hepatectomy in wild type mice treated with SB204741 or ketanserin[19]. Increased liver/body weight ratios were observed up to 7-days post-surgery for SB204741-treated animals compared to vehicle and ketanserin-treated groups (fig 2g), demonstrating sustained stimulation of liver regeneration following selective antagonism of 5-HT_{2B}. Ki67 and PCNA staining revealed increased numbers of proliferating hepatocytes in SB204741-treated livers (fig 2h and supplementary fig 4), by contrast ketanserin reduced numbers of Ki67+ cells confirming a previous report that serotonin stimulates liver regeneration via 5-HT_{2A}[15]. SB204741-treatment also repressed hepatic TGFβ1 expression compared with the control and ketanserin groups where TGFβ1 was elevated at 36 and 72 hrs (fig 2i).

5-HT_{2B} signalling on HSC induces hepatic TGFβ1 and inhibits liver regeneration.

In diseased liver, 5-HT_{2B} is expressed by cholangiocytes and Kupffer cells (KC) as well as by HSC (supplementary fig 5). 5-HT_{2B} was also induced in HSC following partial hepatectomy (fig 3a) whereas expression in hepatocytes was reduced (supplementary fig 6). C1-3-gliotoxin treatment enhanced hepatocyte proliferation following partial hepatectomy and this was accompanied by diminished hepatic expression of TGFβ1 (fig 3b-d). Akin to the BDL model HSC depletion did not affect numbers of F4/80+ Kupffer cells and CK19+ cholangiocytes, and had no impact on progenitor cell proliferation or hedgehog signalling (supplementary fig 7). Given the similarity

between the effects of HSC depletion and antagonism of 5-HT_{2B} on hepatocyte proliferation in multiple injury models it seemed likely that HSC mediate the repressive effects of 5-HT_{2B}. If however HSC depletion and 5-HT_{2B} antagonism influence hepatocyte proliferation via independent mechanisms then combined depletion of HSC and treatment with SB204741 would result in additive effects (fig 3e). This experiment was carried out at 48-hours post-CCl_4 injury when HSC are maximally activated (supplementary fig 8a). We again observed that HSC depletion and 5-HT_{2B} antagonism enhanced hepatocyte proliferation and inhibited TGFβ1 expression with no changes in expression of AFP, CK19, Gli2 or F4/80 (fig 3f, 3g and supplementary fig 8b). Importantly there were no additive effects from combining HSC depletion and 5-HT_{2B} antagonism. Hepatic TGFβ1 is predominantly expressed by HSC and KC. Serotonin treatment of cultured primary mouse HSC induced increased expression of TGFβ1 which was inhibited by SB204741 (fig 3h). By contrast TGFβ1 expression by cultured mouse KC was repressed by 5-HT, and SB204741-treatment prevented this repression but had no direct stimulatory influence (fig 3i). Given the specificity of C1-3 for HSC-derived αSMA+ myofibroblasts our data are strongly indicative of HSC, rather than myofibroblasts of other cellular origins, being the predominant cell type through which 5-HT_{2B} negatively influences hepatocyte proliferation. However, we cannot unequivocally rule out minor contributions from other 5-HT_{2B} expressing cells.

TGFβ1 gene transcription is under the control of AP-1 (Jun/Fos) transcription factors and in activated HSC the predominant AP-1 factor is JunD, which is under the control of ERK-mediated phosphorylation[21-23]. Chromatin immunoprecipitation (ChIP) assays showed that serotonin stimulates recruitment of JunD to AP-1 binding sites in the distal and proximal promoter regions of the TGFβ1 gene in rat and mouse HSC (fig 3j and supplementary fig 9). Antagonism of 5-HT_{2B} suppressed serotonin-induced recruitment of JunD as did treatment of HSC with the ERK inhibitor PD98059. Serotonin stimulated phosphorylation of ERK1/2 in rat (fig 3k), mouse and human HSC

(supplementary fig 10), with this response being inhibited by either PD98059 or SB204741. Serotonin also induced phosphorylation of JunD, which was again suppressed by SB204741 or ERK inhibitor. From these data we propose that intracellular ERK/JunD signalling mediates serotonin/5-HT_{2B} activation of TGFβ1 transcription in HSC (fig 3l). If this pathway operates in the physiological context of the injured liver then JunD would be predicted to function as a transcriptional repressor of hepatocyte proliferation. Analysis of PCNA staining of liver sections from *jund*$^{-/-}$ mice recovering from CCl_4 injury revealed higher numbers of mitotic hepatocytes compared with wild type mice (fig 3m), which was associated with reduced TGFβ1 in *jund*$^{-/-}$ livers (supplementary fig 11). A similar suppressive role of JunD on epithelial cell proliferation has been reported in a model of partial nephrectomy attributed to suppression of TGFα/EGFR signalling on tubular epithelial cells [24].

Antagonism of 5-HT_{2B} attenuates fibrosis and improves liver function.

Recent studies in the kidney suggest that growth arrested epithelial cells stimulate fibrogenesis by secreting TGFβ1 which in this context stimulates the fibrogenic activities of myofibroblasts[25]. We therefore determined if antagonism of 5-HT_{2B} exerts anti-fibrogenic effects in a model of progressive liver disease where both fibrosis and regeneration are actively remodelling the hepatic architecture. Mice received twice weekly CCl_4 injuries for 3-weeks to establish fibrotic disease, prior to injury for further 5-weeks with or without administration of SB204741 (fig 4a). SB204741 significantly reduced numbers of hepatic αSMA+ fibrogenic cells (fig 4b), fibrotic matrix (fig 4c), hepatic expression of TGFβ1 (fig 4d) and expression of the fibrogenic genes, TIMP-1 and pro-collagen I, confirming an anti-fibrogenic effect at the molecular level (fig 4e, f). To corroborate these findings we also determined the effects of SB204741 in the model of progressive BDL-induced liver disease and again observed a protective anti-fibrotic influence (fig 4g) as well as an improvement in liver function as assessed by reduced levels of serum transaminases ALT and AST

(fig 4h). Furthermore, immunohistochemical analysis of caspase 3 activity in the CCl_4 model indicated that SB204741 treatment was associated with higher rates of cellular apoptosis in the fibrotic matrix indicative of enhanced tissue remodelling (supplemental fig 12).

Discussion

Our understanding of the molecular regulation of liver regeneration is mainly derived from studies in "healthy" liver following hepatectomy. Here, we have addressed the additional regulatory complexity that is a feature of regeneration in the context of the diseased liver, and specifically a signalling network established by 5-HT_{2B}-expressing activated HSC which are rare in healthy liver but abundant in diseased liver. It was originally reported that in the healthy liver, platelet-derived serotonin promoted the regenerative response to partial hepatectomy, with this function requiring the activities of the 5-HT_2 subclass of receptors and in particular 5-HT_{2A} which is expressed on hepatocytes[15]. However, expression of 5-HT_{2B} is relatively low in healthy compared to diseased liver, where in the latter it is expressed on activated HSC in association with fibrotic tissue[17]. By focusing on models of progressive liver disease we have discovered that HSC are important suppressors of hepatocyte proliferation and that this function is provided by serotonin-induced expression of TGFβ1 via the 5-HT_{2B} receptor (supplemental fig 13). Moreover, we suggest that this paracrine signalling pathway can feedback onto the HSC to further provoke their fibrogenic activities. 5-HT_{2B} is also selectively expressed by activated human HSC (supplemental fig 14) and the signalling pathway we have described is conserved in human HSC. Antagonists of 5-HT_{2B} are available and safe for use in humans, this class of drug may have exciting therapeutic potential in liver disease, both as a stimulant of hepatocyte regeneration and as an anti-fibrotic.

Acknowledgements.

This work was funded by grants from the UK MRC (grant number G0700890 to DAM, MCW and FO), UK MRC (grant number G0900535 to FO), the Wellcome Trust (grant number WT084961MA to FO, DAM and MCW, and grant WT086755MA to MCW, ADB and DAM). Work in the lab of DAM is also funded by a European Commission FP7 program grant 'INFLA-CARE' (EC Contract No. 223151; http://InflaCare.forth.gr). L. Maroteaux's work has been supported by the Centre National de la Recherche Scientifique, the Institut National de la Santé et de la Recherche Médicale, the Université Pierre et Marie Curie, and by grants from the Fondation de France, the Fondation pour la Recherche Médicale, the French ministry of research (Agence Nationale pour la Recherche), and the European Commission (DEVANX).

Author Contributions.

MRE and FO carried out the majority of the experiments with assistance from LBM, JM, EE, AD, MCW, FJ, AM, MP, AL and LM. AB determined fibrosis scores in the mouse models of liver injury. SAW supplied human liver tissue for isolation of hepatocytes and stellate cells. DAM and FO conceived the study, planned the experiments and wrote the paper.

Figure legends

Figure 1. Selective depletion of hepatic stellate cells or antagonism of 5-HT_{2B} stimulates liver growth.

Mice underwent bile duct ligation (BDL) or sham operation. Fourteen days later BDL mice were given IP injections of C1-3-gliotoxin (C1-3-GT), control antibody conjugated to gliotoxin (CSBD9-GT) or vehicle every other day for a further 7 days. αSMA positive hepatic stellate cells (a), F4/80 positive Kupffer cells (b) and PCNA positive hepatocytes (c) were counted in each group. BrDU immunostained hepatocytes were counted after 14 days BDL ± 5-HT_{2B} antagonist SB204741 (2B), administered daily from day 7 (d). Representative liver sections and

quantification of PCNA positive hepatocytes at 24 hrs after acute CCl_4 liver damage ± 5-HT_{2A} antagonist ketanserin (2A) or the 5-HT_{2B} antagonist SB204741 (2B) (e). Data are expressed as mean ± s.e.m and representative of 5 mice per group. *P <0.05 and **P <0.01 versus control as calculated using ANOVA.

Figure 2. Gene deletion or blockade of 5-HT_{2B} enhances liver regeneration following partial hepatectomy.

Wild type or 5-HT_{2B} receptor knockout mice underwent partial hepatectomy (PHX) or sham operation. Representative liver sections and manual cell counts of PCNA, Ki67 and BrDU immunostained hepatocytes in wild type (WT-black bars) and 5-HT_{2B} receptor knockout (KO-white bars) mice after PHX (a,b,c). Transcript levels of priming cytokines IL-6 and TNF-α were measured in whole liver up to 4 hrs post PHX in WT and KO mice (d,e). Liver TGFβ1 mRNA levels were quantified in KO and WT mice up to 72 hrs post PHX (f). Liver/body weight ratio was calculated in mice treated ± ketanserin (2A) or SB204741 (2B) at 36 hrs, 72 hrs and 7 days after PHX (g). Mitotic hepatocytes were quantified using Ki67 immunostaining at 36 hrs post PHX ± 2A or 2B. Representative liver sections (200x) of liver Ki67 immunostaining (h). Quantitative RT-PCR analysis of whole liver TGFβ1 expression in mice at 36 hrs and 72 hrs post PHX treated ± 2A or 2B (i). Photomicrographs are at 200x magnification. Data are expressed as mean ± s.e.m and representative of at least 4 mice per group. *P <0.05 and **P <0.01 versus control as calculated by ANOVA.

Figure 3. 5-HT_{2B} blockade enhances liver regeneration by inhibiting 5-HT-ERK-JunD dependant induction of TGFβ1 gene expression by HSC.

HSCs were isolated from livers of normal or 36 hrs post partial hepatectomy (PHX) mice and 5-HT_{2B} receptor expression was assessed by immunocytochemistry and quantitative RT-PCR in 3 independent cell preparations (a). Mice underwent PHX and were then given IP injections of C1-3 or C1-3-gliotoxin (C1-3-GT) at 24 hrs and 48 hrs post surgery and then livers were harvested at 72 hrs. PCNA and BrDU positive hepatocytes were counted and TGFβ1 mRNA levels were quantified in C1-3 (Black bars) and C1-3-GT (Grey bars) treated mice (b,c,d). Either depletion of HSC or antagonism of 5-HT_{2B} receptors can promote liver regeneration. $5HT_{2B}$ receptors are expressed on HSC as well as other liver cells and organs. This experiment was performed to determine whether the effect of antagonising 5-HT_{2B} receptors on liver growth is mediated by the HSCs alone or if other liver cells and organs (in addition to the HSC) contribute to this response (e). Top panel - selectively depleting HSC by promoting their apoptosis (AB) or antagonising 5-HT_{2B} receptors expressed on HSCs alone will stimulate liver regeneration (denoted by +). Bottom panel - in addition to effect from HSCs alone (top panel), if other liver cells or organs play a role in liver regeneration through an independent mechanism, then these two separate mechanisms would be additive and generate more liver regeneration (denoted by +++). Mice were injured with CCl_4, then treated at 24 hrs and 40 hrs with either C1-3 or C1-3-GT ± the 5-HT_{2B} antagonist SB204741 (2B) or appropriate vehicle. Livers were harvested at 48 hrs post CCl_4 administration. BrDU positive hepatocytes were counted and TGFβ1 mRNA levels were determined (f,g). Transcript levels of TGFβ1 were assessed in mouse HSC by qRT-PCR (h) or Kupffer cells, KC (i) after 3-6 hrs 5-HT stimulation ± SB204741 (2B). ChIP analysis of JunD recruitment to putative AP-1 sites in the distal region of the TGFβ1 promoter (primer pair 8) in rat HSC stimulated with 5-HT for 4 hrs ± SB204741 or the ERK inhibitor PD98059 (j). Western blot detection of ERK/phospho-ERK, JunD/phospho-JunD and p38/phospho-p38 in rat HSC stimulated with 5-HT for 5 min ± 30 min pre-treatment with PD98059 or SB204741 (k). A schematic representation of ERK dependant recruitment of JunD to the TGFβ1 promoter upon 5-HT binding to 5-HT_{2B} receptor in HSC (l).

PCNA immunostained hepatocytes were quantified in livers of JunD-knockout and wild type mice at peak injury (days 1, 4 and 7 after the final injection) following 8 weeks CCl_4 injury or vehicle (m). Data are expressed as mean ± s.e.m and representative of at least 4 mice per group. *P <0.05 and **P <0.01 and *** P <0.001 versus control as calculated by ANOVA.

Figure 4. Blockade of 5-HT_{2B} receptors attenuates liver fibrosis.

Mice were given CCl_4 IP bi-weekly for 3 weeks then administered SB204741 or vehicle tri-weekly in addition to bi-weekly CCl_4 for a further 5 weeks (a). Average αSMA (HSC marker) immunostained cells in livers after 3 weeks and 8 weeks chronic CCl_4 ± SB204741 and representative αSMA immunostained liver sections after 8 week CCl_4 ± SB204741 (b). Representative sections and fibrosis pathology scoring using the Metavir scale was performed on Sirius Red stained livers (collagen deposition) after 3 weeks or 8 weeks CCl_4 ± SB204741 (c). Quantitative RT-PCR analysis of whole liver TGFβ1, TIMP1 and pro-collagen I after 3 weeks and 8 weeks CCl_4 ± SB204741 (d,e,f). Mice underwent bile duct ligation (BDL) then at 7 days post surgery were given IP injections of SB204741 or vehicle daily for 7 days. Mean liver fibrosis pathology score was performed on Sirius Red stained liver sections (collagen fibres) using the Metavir scale (g). Liver function was assessed in 14 day BDL mice ± 2B by measuring serum transaminases (ALT and AST) (h). All photomicrographs are at 200x magnification. Data are expressed as mean ± s.e.m and representative of 5 mice per group. *P <0.05 and **P <0.01 versus control as calculated by ANOVA.

Supplemental Figures

Supplemental Figure 1. HSC depletion in bile duct ligation does not affect cholangiocyte proliferation or hedgehog signalling.

Mice underwent bile duct ligation (BDL). Fourteen days later BDL mice were given IP injections of C1-3-gliotoxin (C1-3-GT), control antibody conjugated to gliotoxin (CSBD9-GT) or vehicle every other day for a further 7 days. Representative liver sections and morphometric quantification of CK19 and Gli2 positively stained cells shows no difference in the average number of Gli2 and CK19 positively stained cells between the treatment groups. Photomicrographs are at 100-200x magnification. Data are expressed as mean ± s.e.m and representative of 5 mice per group.

Supplemental Figure 2. 5-HT_{2B} receptor antagonism does not affect ductular reaction, progenitor cell proliferation and hepatocyte growth factor expression in liver injury.

Whole liver hepatocyte growth factor (HGF) mRNA levels were measured 24 hrs after acute CCl_4 liver damage ± 5-HT_{2A} antagonist ketanserin (2A) or 5-HT_{2B} antagonist SB204741 (2B) and at 14 days BDL ± the 5-HT_{2B} antagonist SB204741 (2B), administered daily from day 7 (a). Mice underwent bile duct ligation (BDL) or sham operation. At 7 days post surgery mice were given the 5-HT_{2B} antagonist SB204741 (2B) or vehicle daily for 7 days (b). Data shows representative liver sections and morphometric quantification of alpha fetoprotein (AFP), Gli2 and cytokeratin 19 (CK19) positively stained cells. Administration of the 5-HT_2 antagonists did not change hepatic HGF expression or progenitor cell expansion (AFP), hedgehog signalling (Gli2) or cholangiocyte proliferation (CK19). Data are expressed as mean ± s.e.m and representative of 5 mice per group.

Supplemental Figure 3. Deletion of 5-HT_{2B} receptors in mice does not affect liver function.

Serum liver transaminases AST, ALT and gamma-GT (GGT) were similar in normal uninjured adult wild type (WT-white bars) and 5-HT_{2B} receptor knockout (KO-black bars) mice, suggesting that gene deletion of 5-HT_{2B} receptors does not cause liver damage.

Supplemental Figure 4. Selective antagonism of 5-HT_{2B} but not 5-HT_{2A} receptors promote liver regeneration following partial hepatectomy.

Mitotic hepatocytes were quantified using PCNA immunostaining at 36 hrs post PHX ± 2A or 2B receptor antagonist administration. Hepatocyte proliferation was blunted by antagonism of 5-HT_{2A} receptors but stimulated by antagonism of 5-HT_{2B} receptors. Data are expressed as mean ± s.e.m and representative of least 4 mice per group.

Supplemental Figure 5. 5-HT_{2B} receptors expression in normal and diseased liver.

Representative liver sections showing 5-HT_{2B} receptor immuno-histochemical staining in BDL, acute CCl_4 injury, normal liver and the positive control tissues stomach and brain. Red arrows denote HSC and yellow arrows denote cholangiocytes. Photomicrographs are at 200-400x magnification.

Supplemental Figure 6. 5-HT_{2B} receptors expression in hepatocytes isolated from normal and partial hepatectomy liver.

5-HT_{2B} receptor mRNA levels were quantified in isolated hepatocytes, Kupffer cells, cholangiocytes and HSC (a) and hepatocytes isolated from either normal liver or 72 hrs partial hepatectomised liver (PHX) (b). HSC express high levels of 5-HT_{2B} receptor compared to other liver cell types. Hepatocytes express relatively low levels of this receptor and the expression decreases by ~50% after partial hepatectomy.

Supplemental Figure 7. HSC depletion during partial hepatectomy promotes liver regeneration.

Mice underwent PHX and were then given IP injections of C1-3 or C1-3-gliotoxin (C1-3-GT) at 24 hrs and 48 hrs post surgery. The data shows representative liver sections and morphometric

quantification of, AFP, Gli2 and CK19 and total manual cell counts in 15 HP fields of αSMA (HSC), PCNA (hepatocyte regeneration), BrDU and F4/80 (Kupffer Cells) positively stained cells. Administration of C1-3-GT to partial hepatectomised mice resulted in a reduction of αSMA+ cells and an increase in hepatocyte proliferation. However, no change in expansion of hepatic progenitor cells, hedgehog signalling, cholangiocyte proliferation or Kupffer cells was observed. Photomicrographs are at 100-200x magnification. Data are expressed as mean ± s.e.m and representative of 4 mice per group. $*P < 0.05$ and $**P < 0.01$ versus control as calculated by ANOVA.

Supplemental Figure 8. Depletion of HSC or antagonism of 5-HT_{2B} receptors does not affect the liver damage, cholangiocyte or progenitor cell proliferation after toxic injury but stimulates liver regeneration.

Whole liver αSMA mRNA levels, a marker of HSC activation, were quantified in olive oil controls and at 24, 48 and 72 hrs post CCl_4 injury (a) and was maximal at 48 hrs. Representative liver sections and morphometric quantification of AFP (progenitor cells), Gli2 (hedgehog signalling) and CK19 (cholangiocyte proliferation) and total manual cell counts in 15 HP fields of αSMA (HSC), PCNA (hepatocyte regeneration) and F4/80 (Kupffer Cells) positively stained cells in mice injured with CCl_4, then treated at 24 hrs and 40 hrs with either C1-3 or C1-3-GT ± the 5-HT_{2B} antagonist SB204741 (2B) or appropriate vehicle (b). Either HSC depletion (reduced αSMA), administration of the 5-HT_{2B} antagonist SB204741 or these treatments combined stimulated liver regeneration (PCNA) to equivalent levels but does not affect progenitor cell (AFP) or cholangiocyte (CK19) proliferation or Kupffer cells (F4/80) numbers. Photomicrographs are at 100-200x magnification. Serum transaminases ALP, ALT and AST were measured and no difference was observed with administration of either C1-3 or C1-3-GT ± the 5-HT_{2B} antagonist SB204741 (2B), suggesting that the injury process was not affected by 5-HT_{2B} receptor

antagonism or HSC depletion (c). Data are expressed as mean ± s.e.m and representative of 5 mice per group. *P <0.05 and ***P <0.001 versus control as calculated by ANOVA.

Supplemental Figure 9. Selective blockade of 5-HT_{2B} receptor in hepatic stellate cells reduces recruitment of JunD to the mouse and rat TGFβ1 promoter.

ChIP primers were designed to span regulatory AP-1 sites either distal (primer 8 and fig 3j) or proximal (primer 2) to the transcription start site of the rat TGFβ1 gene (a). Data shows recruitment of JunD to the TGFβ1 promoter in serotonin-treated rat HSC. ChIP primers were designed to span regulatory AP-1 sites either distal (primer 1) or proximal (primer 2) to the transcription start site of the mouse TGFβ1 gene (b). ChIP analysis of JunD recruitment to putative AP-1 sites in the distal and proximal regions of the TGFβ1 promoter in mouse HSC stimulated with 5-HT for 4 hrs but not in HSC pre-treated with SB204741 or the ERK inhibitor PD98059 (b).

Supplemental Figure 10. Selective antagonism of 5-HT_{2B} receptor in mouse and human hepatic stellate cells reduces ERK Phosphorylation.

Western blot detection of ERK/phospho-ERK in mouse (a) and human (b) hepatic stellate cells stimulated with 5-HT for 10 min ± 30 min pre-treatment with PD98059 or SB204741.

Supplemental Figure 11. Hepatic TGFβ1 expression is reduced in mice lacking JunD after chronic liver injury.

Whole liver TGFβ1 mRNA levels were quantified in wild type (black bars) and JunD-knockout (white bars) mice at peak injury (day 1 after the final CCl_4 injection), day 4 and 7 following 8 weeks of CCl_4 injury. Expression of hepatic TGFβ1 is lower in mice lacking JunD. Data are expressed as mean ± s.e.m and representative of 4 mice per group.

Supplemental Figure 12. Caspase 3 activity in fibrotic liver treated with serotonin receptor antagonists.

Mice were given CCl_4 by IP injection bi-weekly for 3 weeks then administered ketanserin (2A) or SB204741 (2B) or vehicle was then administered tri-weekly in addition to bi-weekly CCl_4 for a further 5 weeks. Average cell counts of active caspase 3 (apoptotic cells) in livers after 3 and 8 weeks chronic CCl_4 ± ketanserin or SB204741. Antagonism of 5-HT_{2B} receptor but not 5-HT_{2A} receptors significantly increase apoptosis.

Supplemental Figure 13. Regulation of hepatocyte proliferation and fibrogenesis by the 5-HT_2 receptors.

Diagram showing that platelet derived serotonin can directly stimulate hepatocyte regeneration via 5-HT_{2A} receptors expressed on hepatocytes, but simultaneously induce expression of the potent inhibitor of hepatocyte regeneration; TGFβ1 via the 5-HT_{2B} receptor expressed on HSC in an ERK-P – JunD-P dependant manner. We suggest that autocrine TGFβ1 signalling can feedback onto the HSC to further provoke their fibrogenic activities in addition to providing a negative signal to limit liver regeneration.

Supplemental Figure 14. Selective expression of 5-HT_{2B} in human hepatic stellate cells.

Western blot detection of 5-HT_{2B} in primary cell-culture activated human hepatic stellate cells (HSC) and primary human hepatocytes. 5-HT_{2B} receptors are highly expressed in HSC compared to human hepatocytes.

Materials & Methods

Mice and models of liver injury and regeneration. *5-HT$_{2B}^{-/-}* mice were on a 129/PAS background and *JunD*$^{-/-}$ mice were generated on a mixed C57Bl6/129Sv background[23,26]. Aged matched C57Bl6 mice were used for 5-HT$_2$ antagonist studies where mice were administered IP with either SB204741 or ketanserin (3mg/kg bwt, Tocris Biochemicals, UK) or vehicle. Partial hepatectomy (PHX) was performed according to the method of Higgins and Anderson[27], and drugs administered daily in this model with BrdU (150mg/kg bwt) given by IP injection 2 hrs prior to cull. In the PHX ± C1-3 or C1-3-GT model antibodies were administered at 2mg/kg bwt, at 24 and 48 hrs post surgery. Bile duct ligation (BDL) was performed as previously described[28], with SB204741 administered daily from Day 7-14 post-surgery. Targeted hepatic stellate cell depletion during BDL was achieved using C1-3 single chain antibody conjugated to gliotoxin as previously reported[12]. Acute CCl_4 injury - mice were pre-treated for 2 hrs by IP injection of SB204741, Ketanserin or vehicle prior to IP administration of high dose CCl_4 (2µl of CCl_4:Olive oil [1:1 (v/v)]/g bwt). Second doses of 5-HT$_2$ antagonists or vehicle were administered at 22 hrs and mice culled at 24 hrs. In the acute high dose CCl_4 ± C1-3 or C1-3-GT ± SB204741, therapies were given at 24 and 40 hrs post injury. Chronic CCl_4 injury and fibrosis was induced by bi-weekly IP administration of CCl_4 (2µl of CCl_4:Olive oil [1:3 (v/v)]/g bwt) for 8 weeks. From 3 weeks, mice in the 5-HT$_2$ antagonist study, also received tri-weekly IP injections of SB204741 or vehicle.

Primary liver cell isolation and culture. Using the protocol previously reported, HSC were isolated and cultured from male Sprague-Dawley rats and C57Bl6 mice[23,28,29]. Human HSC and hepatocytes were obtained from the normal margins of livers resected for removal of metastatic colo-rectal tumours with full ethical consent of the patient[11]. Early passage HSC were grown to 70-80% confluency in growth medium, at 37^{o}C and 5% CO_2. Unless stated HSC were treated with 100µM SB204741, 5µM serotonin and 25µM ERK inhibitor PD98059. Mouse Kupffer cells (KC) were isolated from livers digested with 20mg collagenase B and 110mg pronase (Roche). Digested

livers were filtered through nybolt and pelleted by centrifugation at 400g for 7 mins. Cell pellets were re-suspended in HBSS containing DNAse, layered onto a 16% Optiprep gradient and spun at 600g for 20 mins. The upper layer containing KC was removed and cells were pelleted as before. KC were re-suspended in medium and plated for 25 mins to allow KC to adhere, plates were washed thoroughly to remove contaminating cells and then KC were cultured at 37^{o}C and 5% CO_2.

Immunohistochemistry was performed on formalin-fixed liver sections. PCNA, BrDU and αSMA was performed as previously described[28]. Endogenous peroxidase activity was blocked and antigen retrieval achieved by citric saline for Ki67, AFP, Gli2, CK19 and active caspase-3. For 5-HT_{2B} receptors combination citric saline and trypsin antigen retrieval was performed followed by permeabilisation with 0.5% Triton. For F4/80 antigen retrieval achieved by proteinase K treatment. Tissue was blocked with Avidin/Biotin Blocking Kit (Vector Laboratories) then 20% swine serum in PBS. Sections were incubated with primary antibodies anti-Ki67 (Novacastra, rabbit, 1:1000), AFP (Dako, rabbit, 1:75), Gli2 (Genway Biotech, rabbit, 1:500), CK19 (Abcam, rabbit, 1:250), 5-HT_{2B} receptors (BD Pharminogen mouse, 1:200), F4/80 (Abcam, rat, 1:100), and active caspase-3 (Cell Signalling Technology, rabbit, 1:200) overnight at 4°C. Sections were incubated with secondary antibody conjugated to biotin (Dako, 1:1000) for 2 hrs, washed then further incubated with Streptavidin Biotin-Peroxidase Complex (Vector Laboratories) and positive cells visualised by 3,3′-diaminobenzidine tetrahydrochloride staining. Manual counts of immunostained cells were calculated as the mean number of positive cells/field in 15-20 high power (20x) fields ± s.e.m. Image analysis was performed using Leica Qwin.

Sirius Red staining. Performed on formalin-fixed liver sections. Tissue was incubated in 0.2% phospho-molybdic acid for 5 mins, in Picro-Sirius Red for 2 hrs and briefly rinsed with 0.01% HCl. Image analysis was performed using Leica Qwin software.

Immunocytochemistry. HSC isolated from C57Bl6 mice injured by PHX were cultured for 2 hrs on cover-slips in a 12 well plate. Cells were formalin-fixed, blocked and incubated with anti-5-HT_{2B} (Acris, rabbit, 1:100) overnight at 4^{o}C. Cells were probed with a mouse anti-rabbit secondary antibody conjugated to Alexafluor-594 for 2 hrs and counterstained with DAPI.

qRT-PCR. Total RNA was isolated from ~200µg mouse liver or cultured cells using the Total RNA Purification Kit (Qiagen). One microgram isolated total RNA was DNAse treated (Promega) and used as template in first strand cDNA synthesis using random primers (Promega). SYBR Green quantitative RT-PCR was performed as previously reported[28].

SDS-PAGE and immunoblotting. Total protein was fractionated by 9% SDS-PAGE and transferred to nitrocellulose. Blots were blocked with TBS/Tween 20 (0.1%, T-TBS) containing 5% bovine serum albumin before overnight incubation with primary antibodies anti-ERK 1&2 and anti-P-ERK 1&2 (Cell Signalling Technology, rabbit, 1:1000), anti-JunD (Santa Cruz, rabbit, 1:500), anti-P-JunD (Upstate, rabbit, 1:500) and anti-$5HT_{2B}$ (BD, mouse, 1:500). Membranes were washed in T-TBS and incubated with either mouse anti-rabbit HRP conjugate (Santa Cruz, 1:2000) or mouse Trueblot (1:5000) for 2 hrs. Blots were washed and antigen detected by ECL (Amersham Biosciences).

Chromatin immunoprecipitation (ChIP) assay. Activated rat or mouse HSC were pre-treated for 30 mins with SB204741 or PD98059 followed by 5-HT stimulation for 4 hrs. Cross-linked chromatin was prepared using the protocol outlined in Upstate Biotechnology Immunoprecipitation (ChIP) assay kit. ChIP was performed on 100µg cross-linked chromatin per reaction. 10µg anti-JunD antibody and non-specific IgG control (Abcam) were used for

immunoprecipitation. PCR amplification of the rat and mouse TGFβ1 promoter was performed using specific oligonucleotide primers (table 1).

Statistical analysis. Data are expressed as means ± standard error of the mean (s.e.m.). GraphPad Instat was used to perform ANOVA with $P< 0.05$ indicative of significance.

References

1. Wallace, K., Burt, A.D. & Wright, M.C. Liver fibrosis. *The Biochemical journal* **411**, 1-18 (2008).
2. Marshall, A., *et al.* Relation between hepatocyte G1 arrest, impaired hepatic regeneration, and fibrosis in chronic hepatitis C virus infection. *Gastroenterology* **128**, 33-42 (2005).
3. Roskams, T. Liver stem cells and their implication in hepatocellular and cholangiocarcinoma. *Oncogene* **25**, 3818-3822 (2006).
4. Malik, R., Selden, C. & Hodgson, H. The role of non-parenchymal cells in liver growth. *Seminars in cell & developmental biology* **13**, 425-431 (2002).
5. Friedman, S.L. Hepatic stellate cells: protean, multifunctional, and enigmatic cells of the liver. *Physiological reviews* **88**, 125-172 (2008).
6. Passino, M.A., Adams, R.A., Sikorski, S.L. & Akassoglou, K. Regulation of hepatic stellate cell differentiation by the neurotrophin receptor p75NTR. *Science* **315**, 1853-1856 (2007).
7. Kalinichenko, V.V., *et al.* Foxf1 +/- mice exhibit defective stellate cell activation and abnormal liver regeneration following CCl4 injury. *Hepatology* **37**, 107-117 (2003).
8. Scobie, B.A. & Summerskill, W.H. Hepatic Cirrhosis Secondary to Obstruction of the Biliary System. *The American journal of digestive diseases* **10**, 135-146 (1965).
9. Polimeno, L., *et al.* Cell proliferation and oncogene expression after bile duct ligation in the rat: evidence of a specific growth effect on bile duct cells. *Hepatology* **21**, 1070-1078 (1995).
10. Wright, M.C., *et al.* Gliotoxin stimulates the apoptosis of human and rat hepatic stellate cells and enhances the resolution of liver fibrosis in rats. *Gastroenterology* **121**, 685-698 (2001).
11. Elrick, L.J., *et al.* Generation of a monoclonal human single chain antibody fragment to hepatic stellate cells--a potential mechanism for targeting liver anti-fibrotic therapeutics. *Journal of hepatology* **42**, 888-896 (2005).
12. Douglass, A., *et al.* Antibody-targeted myofibroblast apoptosis reduces fibrosis during sustained liver injury. *Journal of hepatology* **49**, 88-98 (2008).

13. Cassiman, D., Libbrecht, L., Desmet, V., Denef, C. & Roskams, T. Hepatic stellate cell/myofibroblast subpopulations in fibrotic human and rat livers. *Journal of hepatology* **36**, 200-209 (2002).
14. Omenetti, A., *et al.* Hedgehog-mediated mesenchymal-epithelial interactions modulate hepatic response to bile duct ligation. *Laboratory investigation; a journal of technical methods and pathology* **87**, 499-514 (2007).
15. Lesurtel, M., *et al.* Platelet-derived serotonin mediates liver regeneration. *Science* **312**, 104-107 (2006).
16. Omenetti, A., *et al.* Paracrine modulation of cholangiocyte serotonin synthesis orchestrates biliary remodeling in adults. *American journal of physiology* **300**, G303-315.
17. Ruddell, R.G., *et al.* A role for serotonin (5-HT) in hepatic stellate cell function and liver fibrosis. *The American journal of pathology* **169**, 861-876 (2006).
18. Forbes, I.T., Jones, G.E., Murphy, O.E., Holland, V. & Baxter, G.S. N-(1-methyl-5-indolyl)-N'-(3-methyl-5-isothiazolyl)urea: a novel, high-affinity 5-HT2B receptor antagonist. *Journal of medicinal chemistry* **38**, 855-857 (1995).
19. Varty, G.B. & Higgins, G.A. Reversal of dizocilpine-induced disruption of prepulse inhibition of an acoustic startle response by the 5-HT2 receptor antagonist ketanserin. *European journal of pharmacology* **287**, 201-205 (1995).
20. Fausto, N. Protooncogenes and growth factors associated with normal and abnormal liver growth. *Digestive diseases and sciences* **36**, 653-658 (1991).
21. Kim, S.J., *et al.* Autoinduction of transforming growth factor beta 1 is mediated by the AP-1 complex. *Molecular and cellular biology* **10**, 1492-1497 (1990).
22. Smart, D.E., *et al.* JunD regulates transcription of the tissue inhibitor of metalloproteinases-1 and interleukin-6 genes in activated hepatic stellate cells. *The Journal of biological chemistry* **276**, 24414-24421 (2001).
23. Smart, D.E., *et al.* JunD is a profibrogenic transcription factor regulated by Jun N-terminal kinase-independent phosphorylation. *Hepatology (Baltimore, Md* **44**, 1432-1440 (2006).
24. Pillebout, E., *et al.* JunD protects against chronic kidney disease by regulating paracrine mitogens. *The Journal of clinical investigation* **112**, 843-852 (2003).
25. Yang, L., Besschetnova, T.Y., Brooks, C.R., Shah, J.V. & Bonventre, J.V. Epithelial cell cycle arrest in G2/M mediates kidney fibrosis after injury. *Nature medicine* **16**, 535-543, 531p following 143.
26. Nebigil, C.G., *et al.* Serotonin 2B receptor is required for heart development. *Proceedings of the National Academy of Sciences of the United States of America* **97**, 9508-9513 (2000).
27. Higgens & RA, A. Restoration of the liver of white rat following partial surgical removal. *Arch Pathol* **12**, 186 (1931).
28. Gieling, R.G., *et al.* The c-Rel subunit of nuclear factor-kappaB regulates murine liver inflammation, wound-healing, and hepatocyte proliferation. *Hepatology* **51**, 922-931.
29. Arthur, M.J., Friedman, S.L., Roll, F.J. & Bissell, D.M. Lipocytes from normal rat liver release a neutral metalloproteinase that degrades basement membrane (type IV) collagen. *The Journal of clinical investigation* **84**, 1076-1085 (1989).

Figure 1

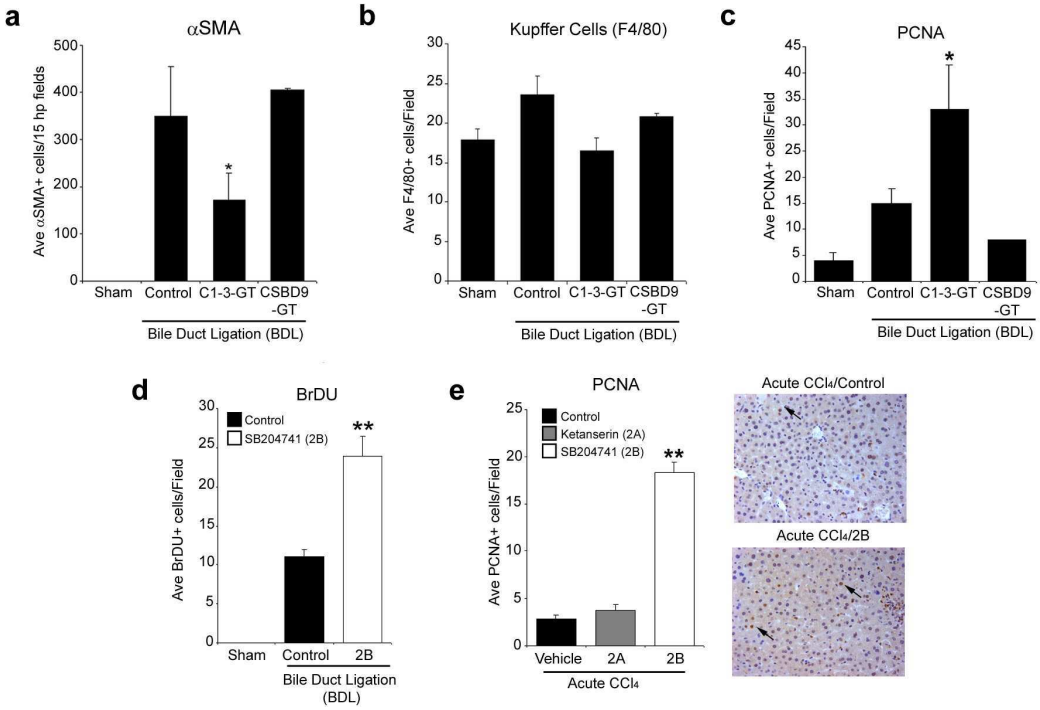

Figure 2

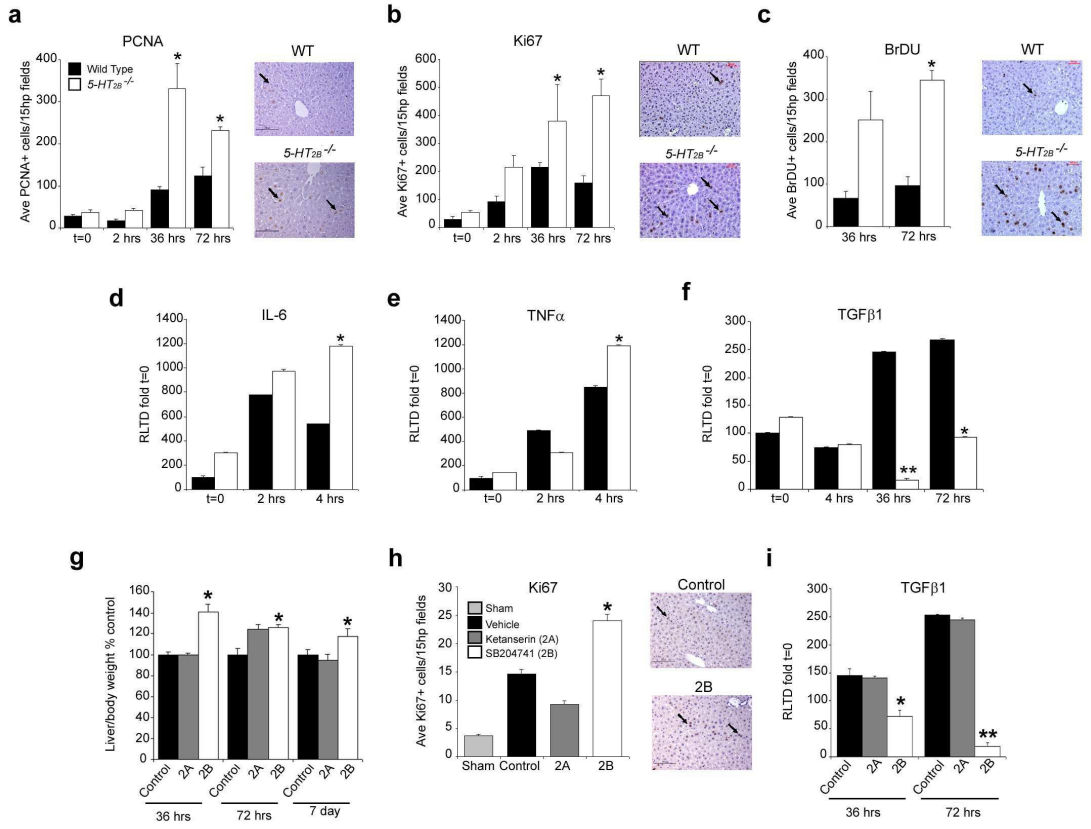

Figure 3

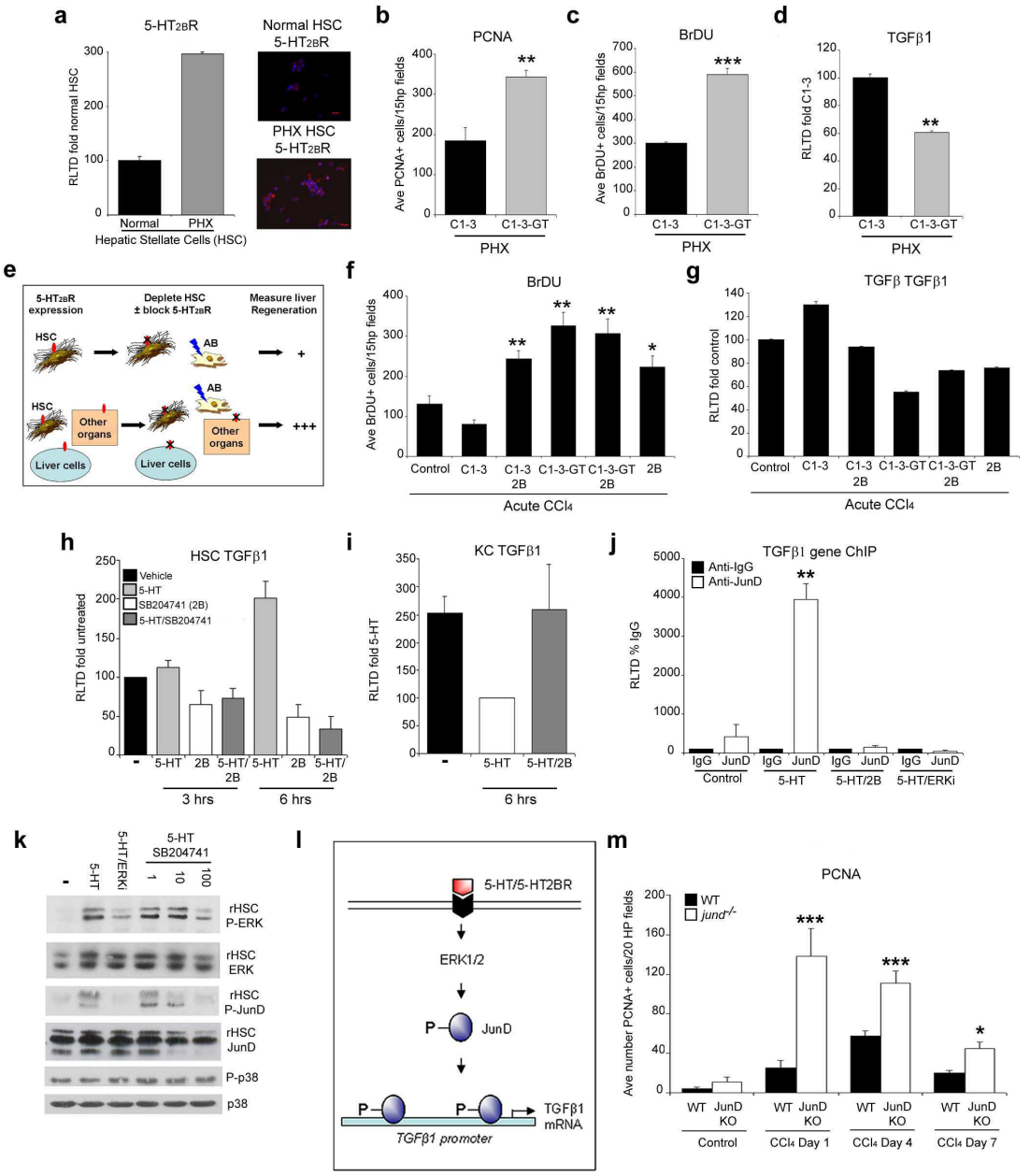

Figure 4

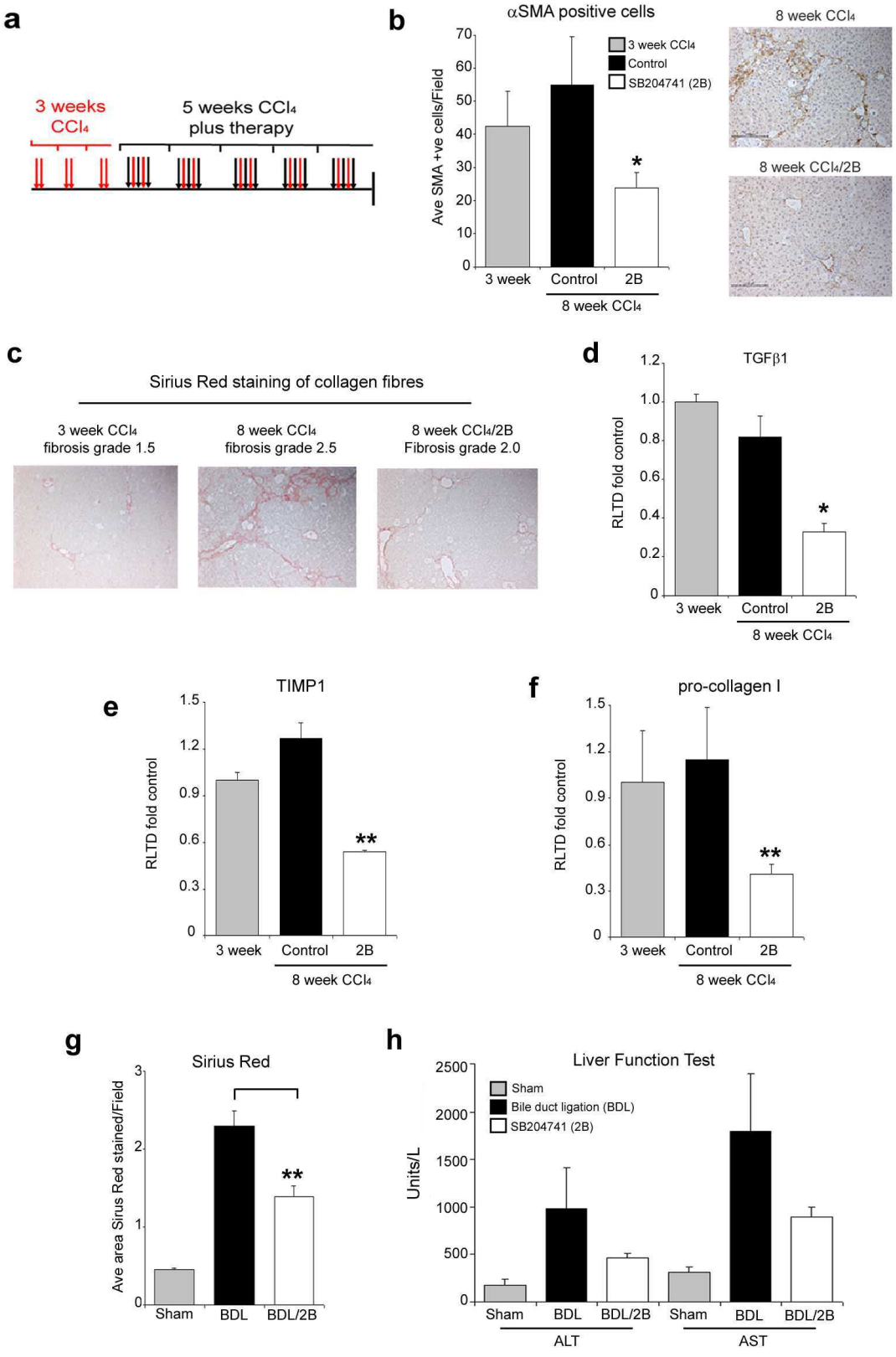
a
3 weeks CCl4
5 weeks CCl4 plus therapy
b
αSMA positive cells
3 week CCl4
Control
SB204741 (2B)
Ave SMA +ve cells/Field
3 week
Control
2B
8 week CCl4
8 week CCl4
8 week CCl4/2B
c
Sirius Red staining of collagen fibres
3 week CCl4 fibrosis grade 1.5
8 week CCl4 fibrosis grade 2.5
8 week CCl4/2B Fibrosis grade 2.0
d
TGFβ1
RLTD fold control
e
TIMP1
f
pro-collagen I
g
Sirius Red
Ave area Sirius Red stained/Field
Sham
BDL
BDL/2B
h
Liver Function Test
Sham
Bile duct ligation (BDL)
SB204741 (2B)
Units/L
ALT
AST

Suppl 1

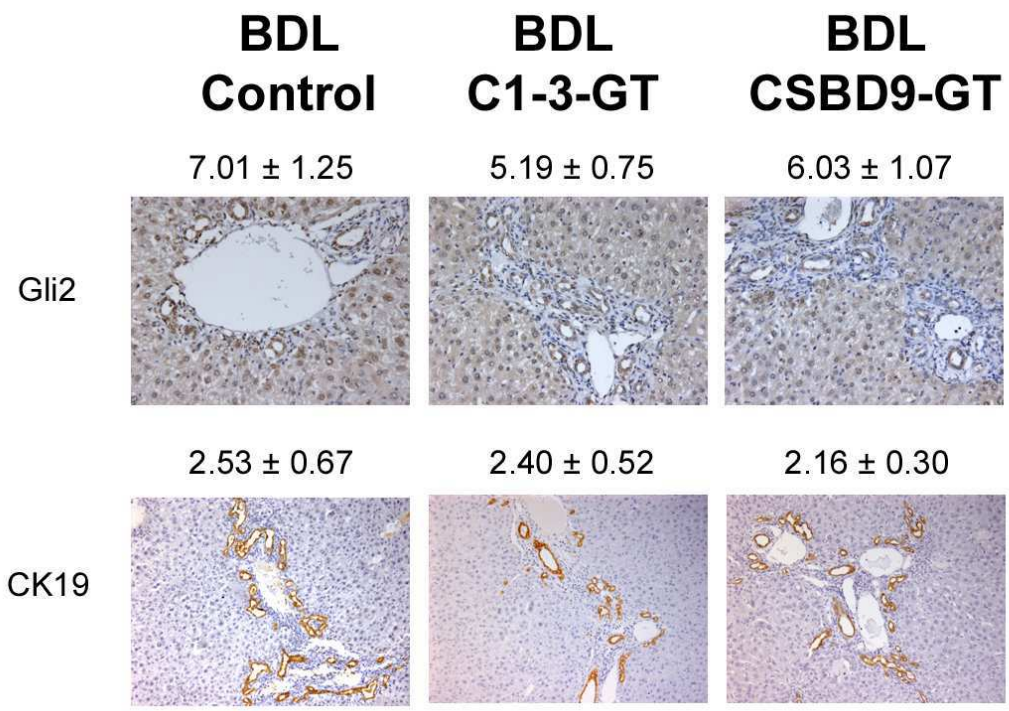
BDL Control
BDL C1-3-GT
BDL CSBD9-GT
7.01 ± 1.25
5.19 ± 0.75
6.03 ± 1.07
Gli2
2.53 ± 0.67
2.40 ± 0.52
2.16 ± 0.30
CK19

Suppl 2

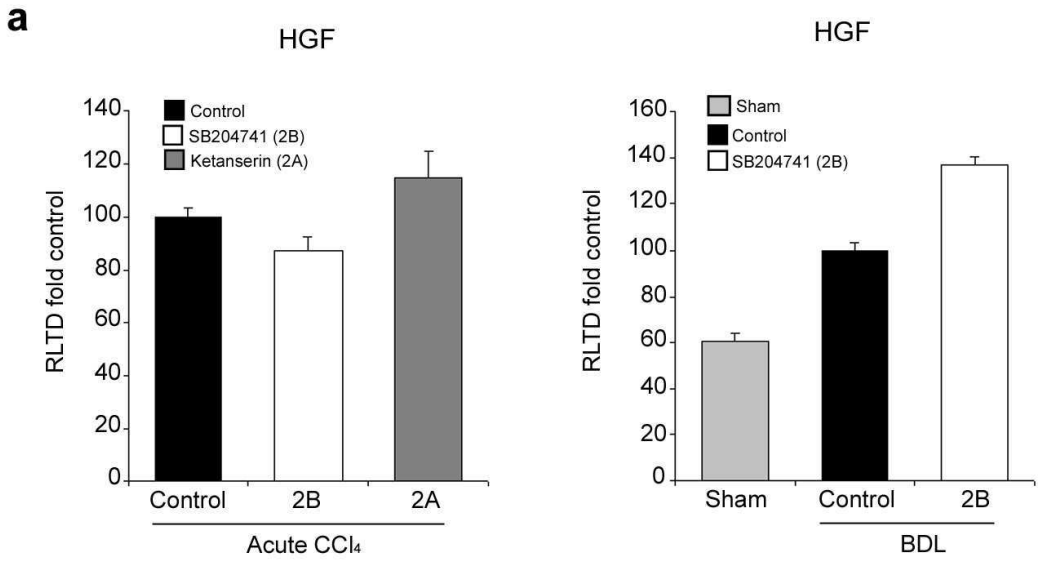
a
HGF
Control
SB204741 (2B)
Ketanserin (2A)
RLTD fold control
140
120
100
80
60
40
20
0
Control
2B
2A
Acute CCl4
HGF
Sham
Control
SB204741 (2B)
RLTD fold control
160
140
120
100
80
60
40
20
0
Sham
Control
2B
BDL

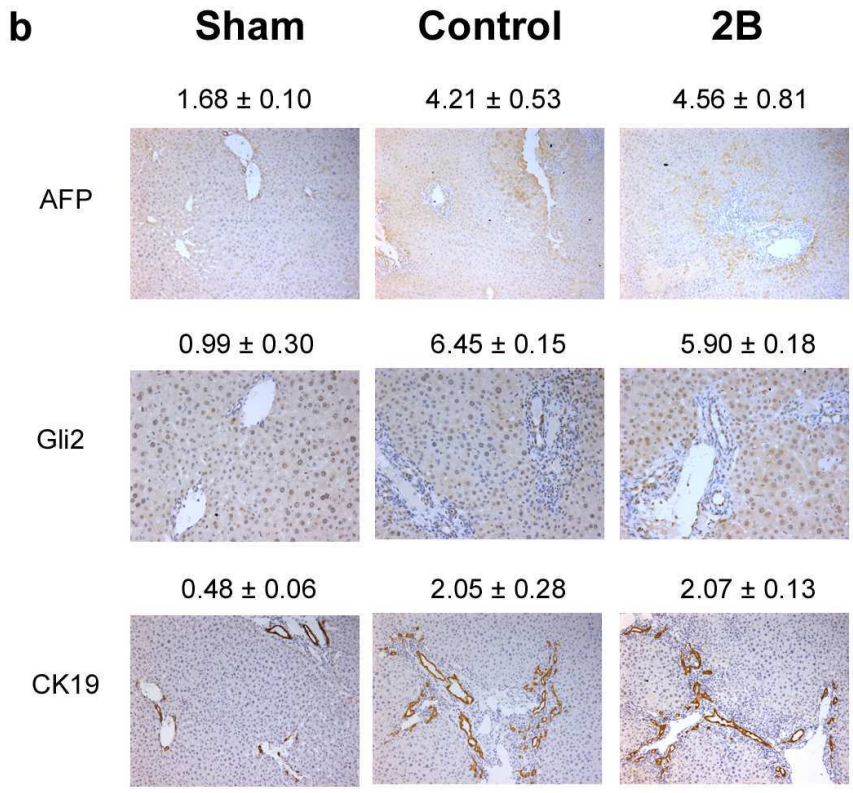
b
Sham
Control
2B
1.68 ± 0.10
4.21 ± 0.53
4.56 ± 0.81
AFP
0.99 ± 0.30
6.45 ± 0.15
5.90 ± 0.18
Gli2
0.48 ± 0.06
2.05 ± 0.28
2.07 ± 0.13
CK19

Suppl 3

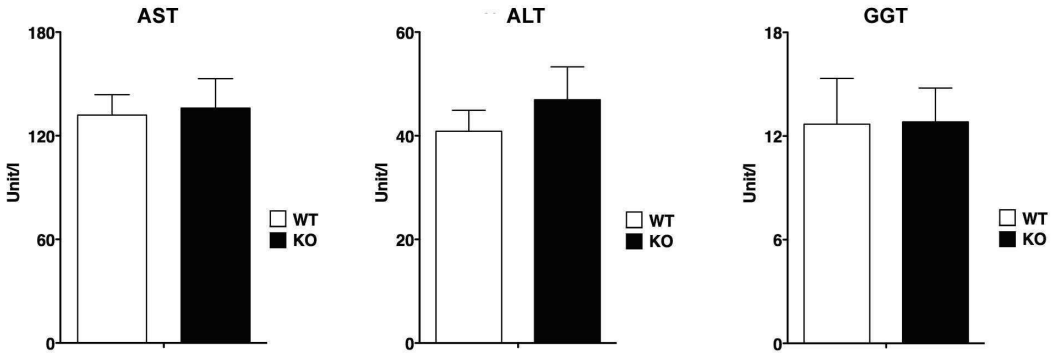

Suppl 4

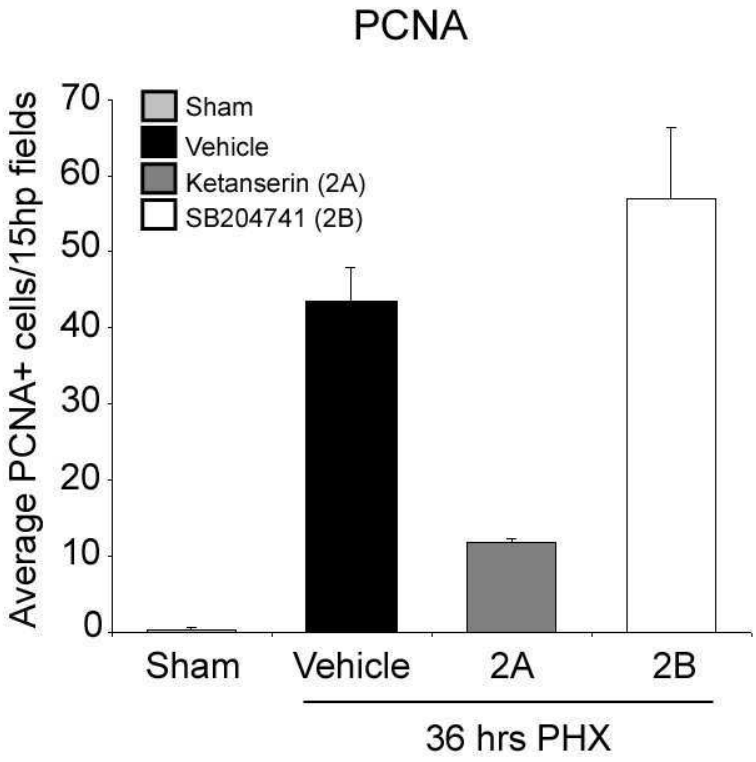

Suppl 5

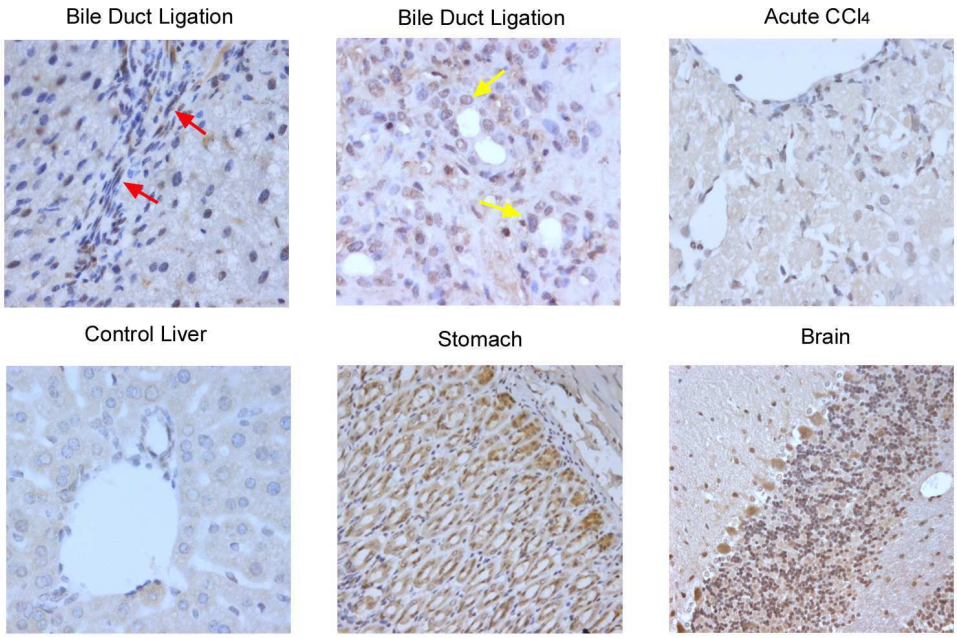

Suppl 6

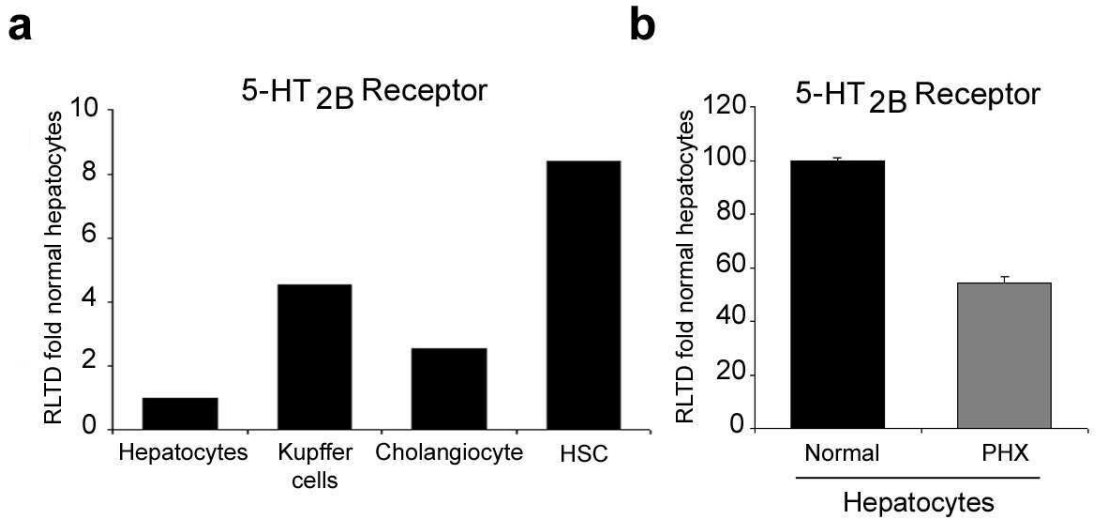

Suppl 7

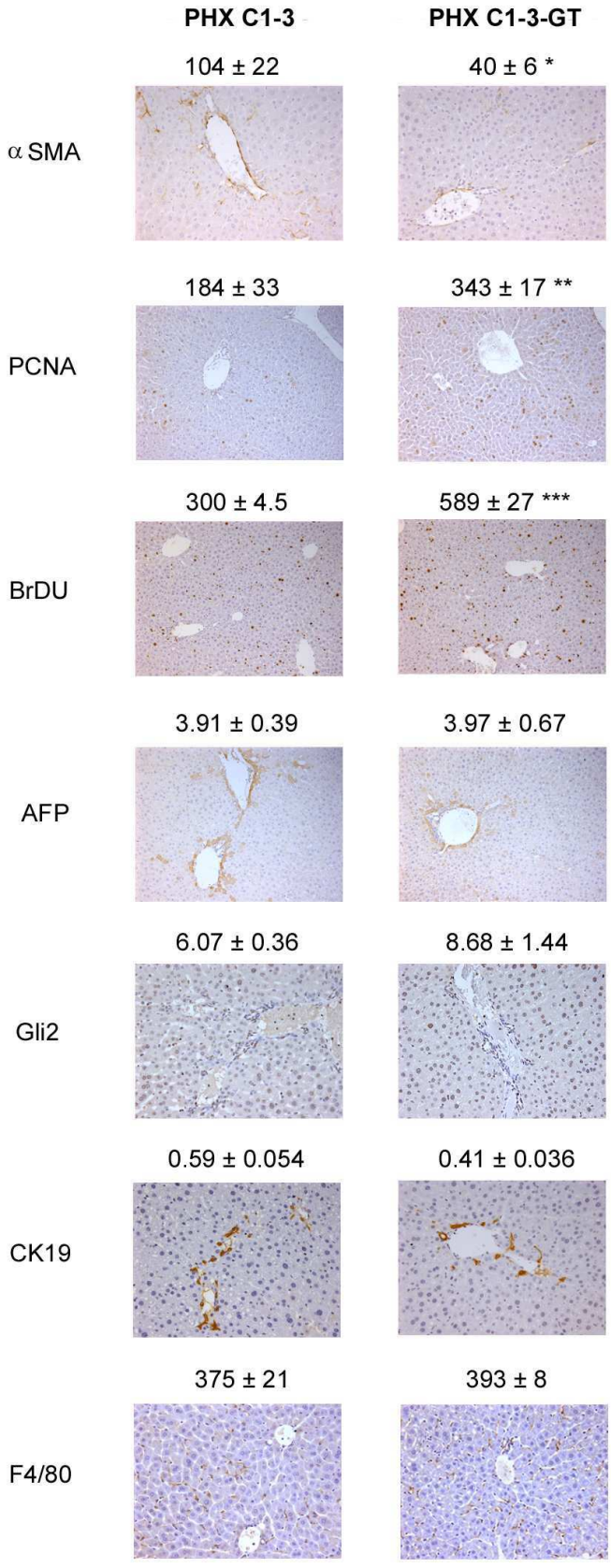
PHX C1-3
PHX C1-3-GT
104 ± 22
40 ± 6 *
α SMA
184 ± 33
343 ± 17 **
PCNA
300 ± 4.5
589 ± 27 ***
BrDU
3.91 ± 0.39
3.97 ± 0.67
AFP
6.07 ± 0.36
8.68 ± 1.44
Gli2
0.59 ± 0.054
0.41 ± 0.036
CK19
375 ± 21
393 ± 8
F4/80

Suppl 8

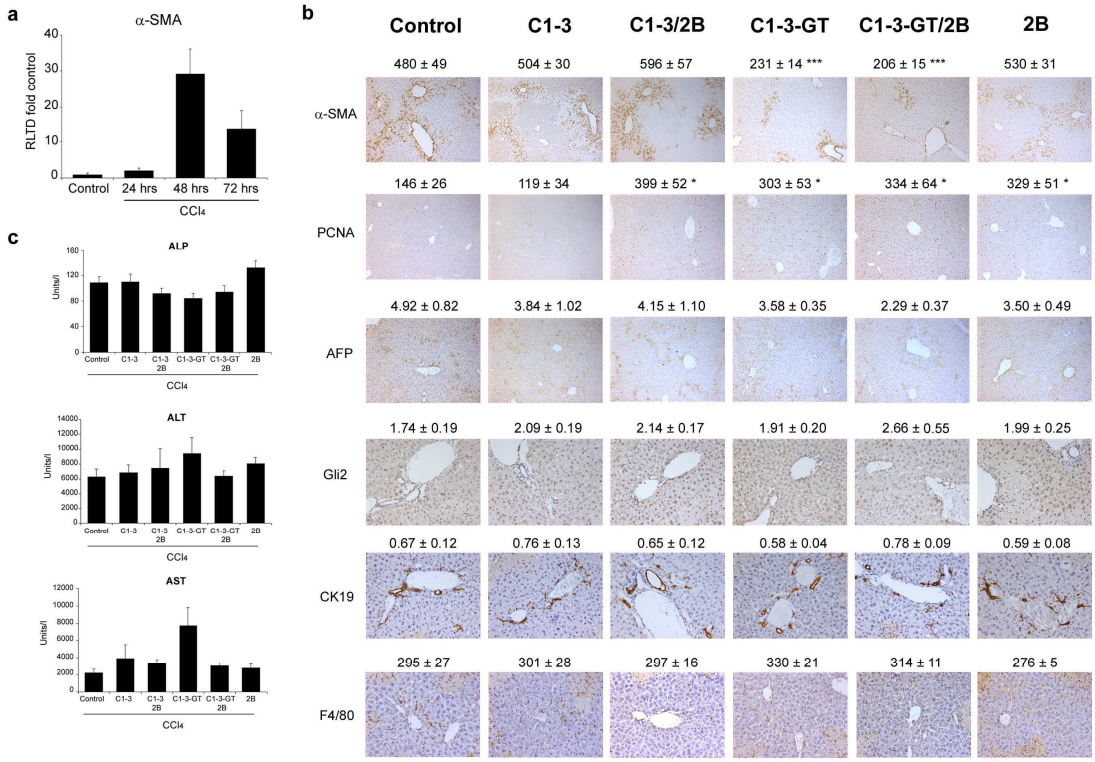
a
α-SMA
RLTD fold control
Control
24 hrs
48 hrs
72 hrs
CCl4
b
Control
C1-3
C1-3/2B
C1-3-GT
C1-3-GT/2B
2B
α-SMA
480 ± 49
504 ± 30
596 ± 57
231 ± 14 ***
206 ± 15 ***
530 ± 31
PCNA
146 ± 26
119 ± 34
399 ± 52 *
303 ± 53 *
334 ± 64 *
329 ± 51 *
AFP
4.92 ± 0.82
3.84 ± 1.02
4.15 ± 1.10
3.58 ± 0.35
2.29 ± 0.37
3.50 ± 0.49
Gli2
1.74 ± 0.19
2.09 ± 0.19
2.14 ± 0.17
1.91 ± 0.20
2.66 ± 0.55
1.99 ± 0.25
CK19
0.67 ± 0.12
0.76 ± 0.13
0.65 ± 0.12
0.58 ± 0.04
0.78 ± 0.09
0.59 ± 0.08
F4/80
295 ± 27
301 ± 28
297 ± 16
330 ± 21
314 ± 11
276 ± 5
c
ALP
Units/l
CCl4
ALT
Units/l
CCl4
AST
Units/l
CCl4

Suppl 9

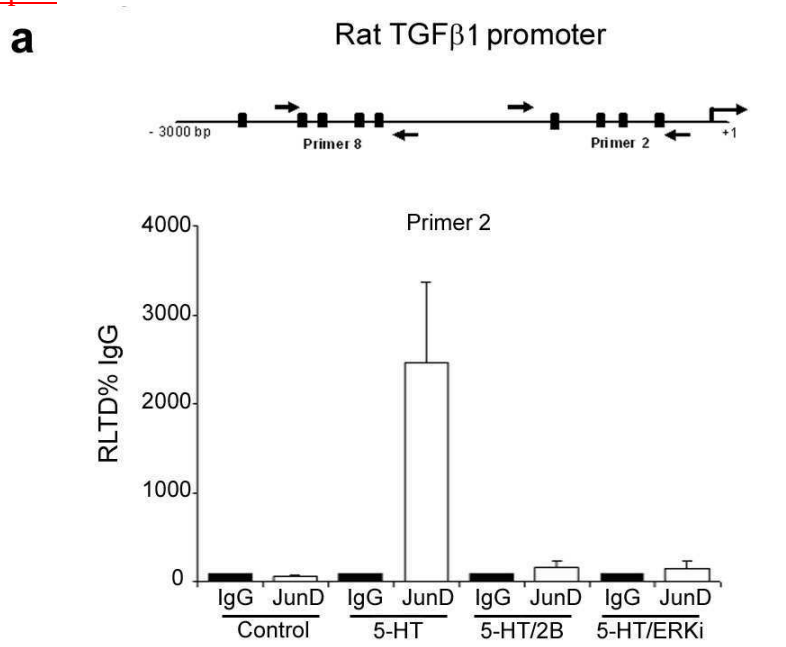
a
Rat TGFβ1 promoter
- 3000 bp
Primer 8
Primer 2
+1
Primer 2
RLTD% IgG
4000
3000
2000
1000
0
IgG JunD IgG JunD IgG JunD IgG JunD
Control
5-HT
5-HT/2B
5-HT/ERKi

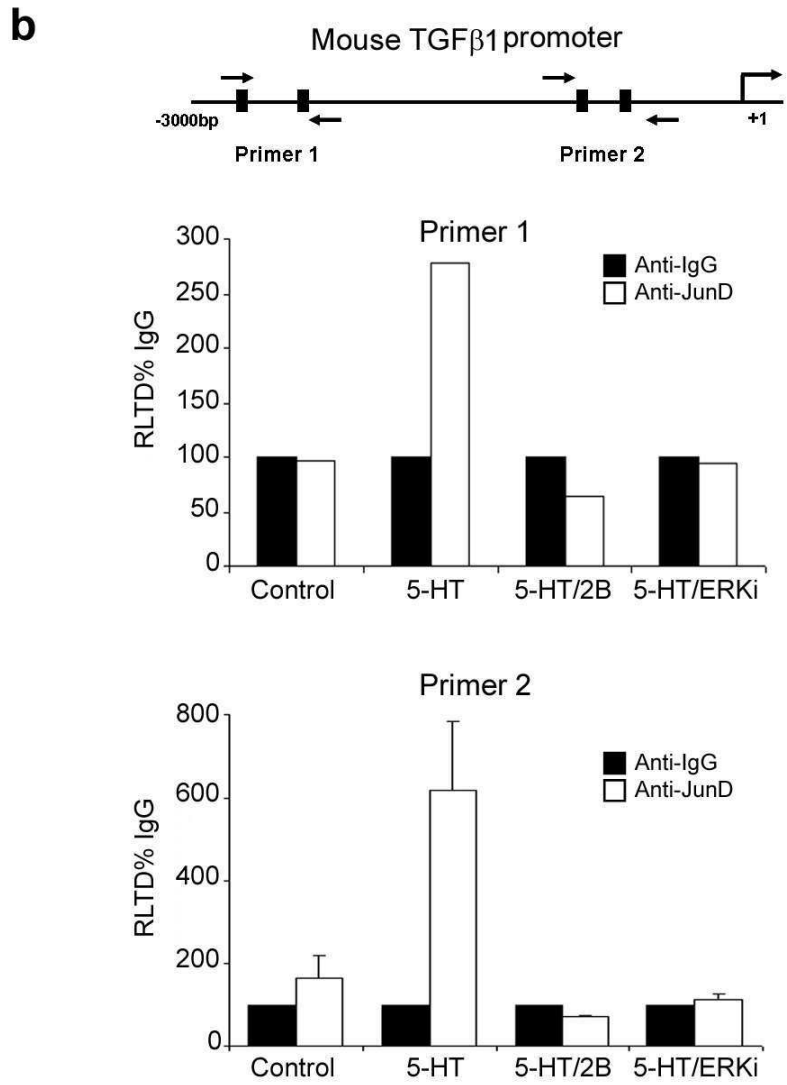
b
Mouse TGFβ1 promoter
-3000bp
+1
Primer 1
Primer 2
Primer 1
RLTD% IgG
300
250
200
150
100
50
0
Anti-IgG
Anti-JunD
Control
5-HT
5-HT/2B
5-HT/ERKi
Primer 2
RLTD% IgG
800
600
400
200
0
Anti-IgG
Anti-JunD
Control
5-HT
5-HT/2B
5-HT/ERKi

Suppl 10

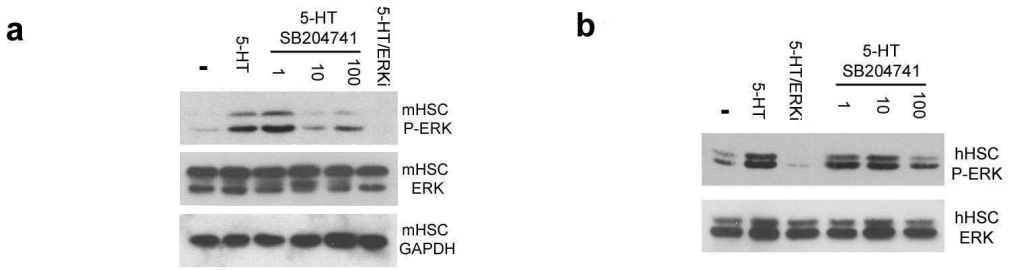

Suppl 11

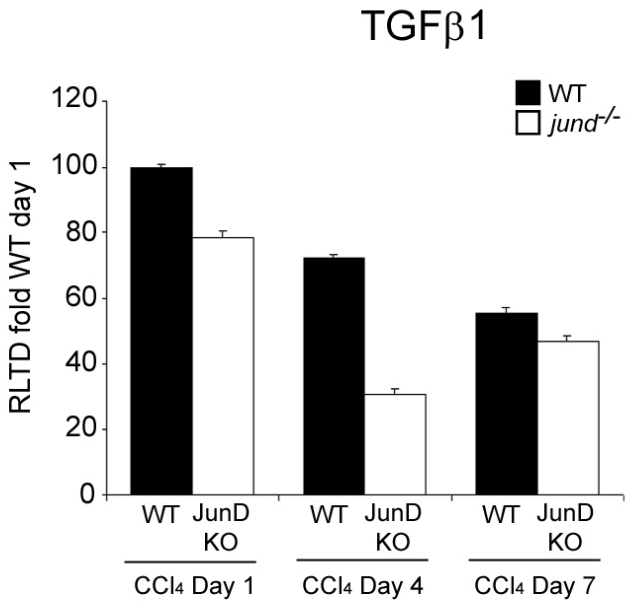

Suppl 12

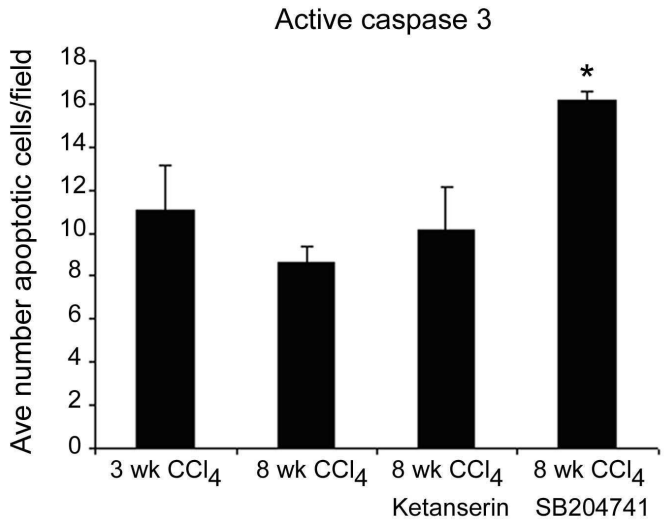
Active caspase 3
Ave number apoptotic cells/field
18
16
14
12
10
8
6
4
2
0
*
3 wk CCl4
8 wk CCl4
8 wk CCl4
Ketanserin
8 wk CCl4
SB204741

Suppl 13

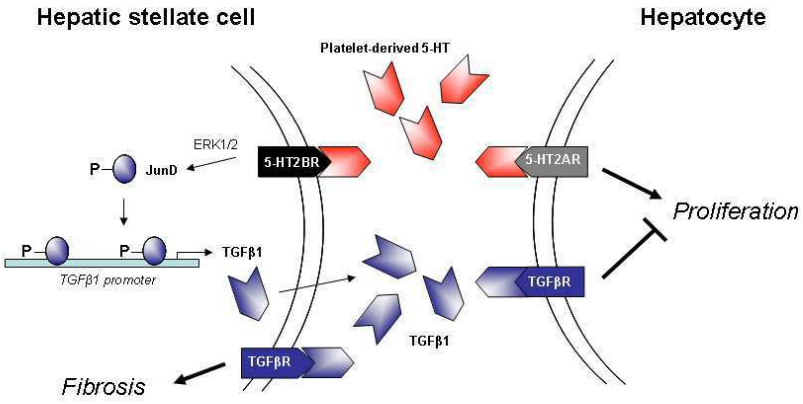
Hepatic stellate cell
Hepatocyte
Platelet-derived 5-HT
ERK1/2
P
JunD
5-HT2BR
5-HT2AR
Proliferation
P
P
TGFβ1
TGFβ1 promoter
TGFβR
TGFβ1
TGFβR
Fibrosis

Suppl 14